Journal of Physics:
Conference Series

PAPER • **OPEN ACCESS**

Impact of minute-time-scale kinetics on the stabilization of the skyrmion-lattice in Cu_2OSeO_3

To cite this article: Johannes D Reim *et al* 2017 *J. Phys.: Conf. Ser.* **828** 012004

IOP Conf. Series: Journal of Physics: Conf. Series **828** (2017) 012004 doi:10.1088/1742-6596/828/1/012004

Impact of minute-time-scale kinetics on the stabilization of the skyrmion-lattice in Cu_2OSeO_3

Johannes D Reim[1], Koya Makino[1], Daiki Higashi[1], Yusuke Nambu[2], Daisuke Okuyama[1], Taku J Sato[1], Elliot P Gilbert[3], Norman Booth[3], and Shinichiro Seki[4,5]

[1]Institute of Multidisciplinary Research for Advanced Materials, Tohoku University, 2-1-1 Katahira, Sendai 980-8577, Japan
[2]Institute for Materials Research, 2-1-1 Katahira, Tohoku University, Sendai 980-8577, Japan
[3]Australian Centre for Neutron Scattering, Australian Nuclear Science and Technology Organization, Kirrawee DC, New South Wales 2232, Australia
[4]RIKEN Center for Emergent Matter Science (CEMS), Wako, Saitama 351-0198, Japan
[5]PRESTO, Japan Science and Technology Agency (JST), Tokyo 102-8666, Japan

E-mail: j.reim@tagen.tohoku.ac.jp

Abstract. Using small angle neutron scattering measurements, we have previously demonstrated the influence of field-cooling (FC), field-warming (FW) and zero-field-cooling (ZFC) protocols on the thermodynamical stability of the skyrmion-lattice phases SkX(1) and SkX(2) in Cu_2OSeO_3. Here, we have discovered that small variations in these protocols can have a significant impact on the phase stabilization. Using the ZFC protocol the stabilization of either SkX(1) or SkX(2) can be tuned either by applying the magnetic field directly or with intermediate steps. Furthermore, introducing waiting times at intermediate temperature steps into the FC and FW protocol significantly influences the skyrmion-lattice stabilization. Although for the latter FC and FW experiment, the extrinsic temperature equilibration effect cannot be excluded, the influence of the temperature and magnetic field sweep rate indicates the importance of slow kinetics on the order of a few minutes for the stabilization process.

1. Introduction

In recent years the research of chiral magnets has attracted considerable interest, as certain compounds exhibit topologically protected swirlings called skyrmions characterized by a topological quantum number [1, 2]. Besides their intriguing nature these entities offer properties well suited for application in information technology. Lattices formed from such skyrmions have been first observed in the chiral helimagnet MnSi [3] and subsequently in numerous ferromagnetic compounds such as FeGe [4], (Fe,Co)Si [5], Cu_2OSeO_3 [6, 7], $Co_8Zn_8Mn_4$ [8] and GaV_4S_8 [9]. The presence of a skyrmion lattice in Cu_2OSeO_3 was evidenced using small angle neutron scattering (SANS) [6, 7] and Lorentz microscopy [10]. As an insulator this compound is quite unusual among those hosting a skyrmion lattice and attracts particular interest due to the resulting multiferroic nature [10, 11]. Recently, we have reported on the thermodynamic stability of skyrmion phases in Cu_2OSeO_3. We were able to relate deviations concerning the stabilization of skyrmion-lattice phases, i.e., the skyrmion-lattice 1 [SkX(1)] and skyrmion-lattice 2 [SkX(1)], in phase diagrams of earlier reports to the difference in temperature (T) and field (H) protocols [12].

These skyrmion-lattice phases are related by a 30° rotation with each other [6]. Cooling the sample in an applied field (FC) stabilizes the SkX(2) phase, while SkX(1) is mostly prominent for field-warming (FW). Following a zero-field-cooling (ZFC) procedure, the SkX(1) and SkX(2) phases are stabilized in coexistence and show no sign of relaxation behavior favoring one of these phases at any point of the phase diagram. This observation indicates an intriguing phase stability most likely due to their topological nature.
Here, we investigate the different protocols in further detail. In the case of the FC and FW protocol, the temperature of the sample changes while traversing the skyrmion phase, whereas in the ZFC protocol the magnetic field is changed. In the paramagnetic (or helical/cycloidal) phase, the system is most likely independent of the path traversed by performing these changes, at least if the path is contained in the respective phase. However, in the skyrmion phase, a path-dependence is present as shown by the difference in stabilization depending on the protocol. In the following, we study the influence of introducing waiting times at intermediate steps which allow for a short time relaxation (up to four minutes) while maintaining the path itself.

2. Experimental

To investigate the structure of the skyrmion lattice in Cu_2OSeO_3, small angle neutron scattering experiments were performed on a high quality single crystal. This crystal with the approximate dimensions 8 mm × 5 mm × 3 mm has been synthesized using the chemical vapor transport method [13]. Neutron experiments were conducted at the beam line QUOKKA [14] located at the OPAL reactor of Australian Nuclear Science and Technology Organization at a wavelength $\lambda \sim 5$ Å and wavelength distribution $\mathrm{d}\lambda/\lambda \sim 10\%$. The skyrmion lattice was stabilized using a closed-cycle ^{4}He refrigerator and an external 5 T horizontal field superconducting magnet with its field aligned parallel to the incident neutron beam $\vec{k}_i$. The sample was placed on a sapphire sample plate with its [110] axis parallel to the incident neutron beam $\vec{k}_i$, and with its [001] axis along the horizontal direction. The scattering background was estimated using the SANS pattern measured at the paramagnetic temperature 60 K, and subsequently subtracted from the data shown here. The rod-shaped Bragg peaks of the skyrmion lattice enable measurement of the scattering intensity of all peaks simultaneously despite the curvature of the Ewald sphere.

3. Results and discussion

The two-dimensional scattering patterns measured in the SANS experiment show a set of two (helical), six [either SkX(1) or SkX(2)] or 12 Bragg reflections [coexistence and thus superposition of SkX(1) and SkX(2)] distributed at $|\vec{Q}| = Q = 0.01$ Å^{-1}. Figure 1(a) and (b) shows exemplary scattering patterns of superimposed skyrmion-lattice phases SkX(1) and SkX(2) stabilized using the ZFC protocol. The observed peak sets depend on the used protocol and the position in the T-H phase diagram. In order to investigate the stabilization of SkX(1) and SkX(2) quantitatively, the scattering pattern is integrated along $\vec{Q}$ for $0.076 \leq Q \leq 0.0124$ Å^{-1}. The resulting pattern displays the dependence of the intensity on the azimuthal angle ϕ. A fit function, consisting of a Gaussian function for each Bragg reflection, was used to extract the intensity, width and position of the peaks belonging to the SkX(1) and SkX(2) phases. Simultaneously, a constant term independent of ϕ was optimized which is related to a ring-like diffuse scattering. A detailed description of the fitting procedure can be found in [12]. While the parameters were optimized for each Friedel pair of scattering peaks individually, in the following, the intensity of SkX(1) and SkX(2) refers to the integrated intensity of all six respective peaks.

3.1. Impact of magnetic field sweep rate on skyrmion-lattice stabilization

In the case of the ZFC protocol, the change of the magnetic field takes place within the skyrmion phase in contrast to the FC and FW protocols. In order to reveal a sweep rate dependence,

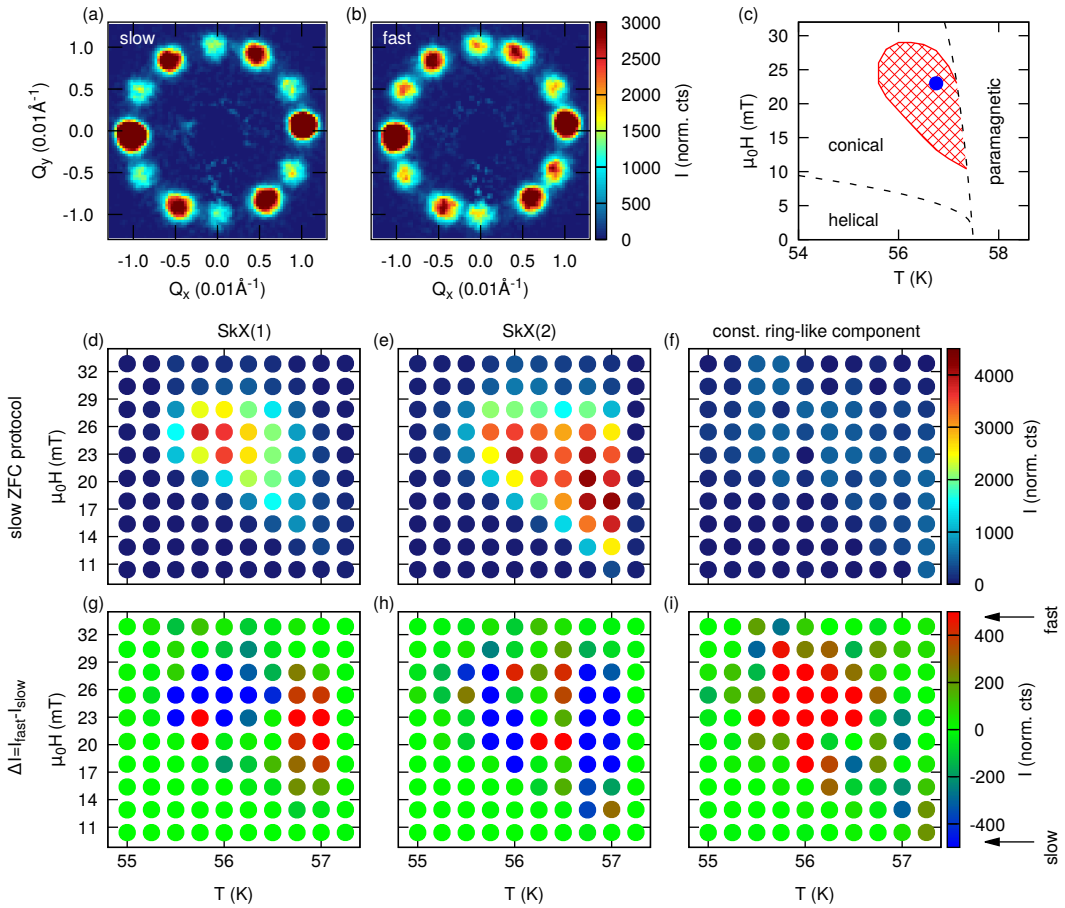

Figure 1. Comparison of the slow and fast ZFC protocol. The scattering pattern measured at $\mu_0 H = 23\,\mathrm{mT}$ and $T = 56.75\,\mathrm{K}$ for the slow (a) and fast (b) ZFC protocol. (c) Schematic phase diagram close to the skyrmion phase (red) and the position of the scattering patterns (a) and (b) within (blue dot). (d-f) Two-dimensional intensity maps for the SkX(1), SkX(2) and the constant ring-like component, obtained by fitting a model function to the scattering pattern. The position of each dot denotes the temperature and field of the associated measurement. (g-i) The color represents the difference in the respective intensity between the fast and slow protocol. The intensity (f) and difference (i) of the ring-like component were scaled by a factor 10.

two different ZFC protocols were used. The first one, described in [12], heats the sample up to $T = 60\,\mathrm{K}$ and cools it down to the target temperature in zero magnetic field. Subsequently, the target magnetic field is always set from the helical phase at $\mu_0 H = 0\,\mathrm{mT}$ using a rate of $23.8\,\mathrm{mT/s}$. This will here be referred to as the "fast" protocol. In the second protocol the magnetic field is increased in steps of $\mu_0 \Delta H = 2.5\,\mathrm{mT}$ starting at $\mu_0 H = 0$ up to $40\,\mathrm{mT}$. The latter protocol is described in Appendix A and will be referred to as the "slow" protocol. After reaching the target field using either of the ZFC protocols the scattering is measured for $60\,\mathrm{s}$. The scattering patterns in figure 1 display skyrmion-lattices stabilized using the slow (a) and fast (b) protocol. While both show Bragg reflections of the skyrmion-lattice phases SkX(1) and dominant SkX(2), there are differences in the intensity ratio of these phases. At this point in the T-H phase diagram [cf. figure 1(c)] the fast protocol enhances SkX(1) in favor of SkX(2). The intensity for the SkX(1), SkX(2) and ring-like diffuse component was determined by fitting the diffraction patterns measured at various T and H. The results of the slow protocol are plotted

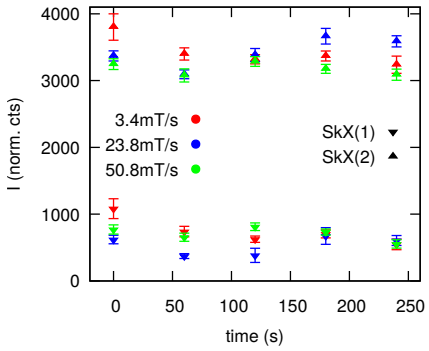

Figure 2. Time evolution of the integrated intensity for the SkX(1) and SkX(2) components applying the fast ZFC protocol. The protocol was performed using different rates for the increase of the magnetic field at $T = 57.0\,\mathrm{K}$. The measurement of the time evolution was started after reaching the target field $\mu_0 H = 20.4\,\mathrm{mT}$.

in 2D maps as a function of T and H [cf. figure 1(d-f)]. The overall structure is rather similar to the intensity maps observed for the fast protocol (see [12]), with SkX(1) being stabilized at lower-T and SkX(2) being dominant in a large area of the skyrmion phase especially at higher-T.

Figures 1(g-i) display the difference in the integrated intensities of SkX(1), SkX(2) and the ring-like component between the fast and slow protocol. The constant component is related to short-range ordered skyrmion-lattices and a large region of the skyrmion-lattice phase (below $T = 56.75\,\mathrm{K}$ and above $\mu_0 H \sim 21\,\mathrm{mT}$) exhibits a consistently greater constant component for the fast protocol. The effect leading to the system becoming kinetically trapped is reduced for either a sufficiently slow increase of the magnetic field, or close to the phase boundary where even shorter waiting times are sufficient for the whole system to become ordered. Looking at the difference in integrated intensities of SkX(1) and SkX(2), the fast protocol stabilizes SkX(1) in favor of SkX(2) close to the skyrmion phase boundary at $T = 57.25\,\mathrm{K}$ in comparison to the slow protocol. This is quite intriguing; while SkX(2) is energetically favored close to this phase boundary, its stabilization can apparently be influenced by changing the field increase procedure. At intermediate temperatures the fast protocol stabilizes the SkX(2) slightly more compared to the slow one. However, using the slow protocol SkX(1) is stabilized more strongly in the region below $T = 56.75\,\mathrm{K}$ and above $\mu_0 H = 23\,\mathrm{mT}$, and SkX(2) below $T = 56.25\,\mathrm{K}$. Since no relaxation of the integrated intensities was observed for both skyrmion-lattices after reaching the target magnetic field, both protocols result in stable configurations. At the same time the structure of the skyrmion-lattice is the same for both protocols, as no significant deviation of the peak widths nor position in Q (i.e. the extent of long-range order and its periodicity) were identified here. Furthermore, the peak sets of SkX(1) and SkX(2) both appear to retain the six-fold symmetry, neither the slow nor the fast protocol introduces a distortion to the skyrmion-lattices.
There have been recent reports on skyrmions forming a glassy structure in the vicinity of the lower-H phase boundary [15, 16]; consequently the related dislocations would remain even in the long-range-ordered skyrmion-lattice phase. The increase of the constant component observed at intermediate H and T using the fast protocol supports the assumption of a glassy state. Furthermore, low diffuse scattering is exhibited using the slow protocol and close to the phase boundary; this corresponds with the glassy state growing into a well-ordered skyrmion-lattice. However, so far this model does not offer a compelling explanation for the T and H-dependence of the stabilization of the SkX(1) and SkX(2) phases respectively.

As the magnetic field sweep rate plays a significant role, at $T = 57.0\,\mathrm{K}$, the fast protocol was used with three different rates (3.4, 23.8 and 50.8 mT/s) by which the magnetic field is increased to reach the target field $\mu_0 H = 20.4\,\mathrm{mT}$. With the slow protocol the target field is reached after $\sim$640 s, which is equivalent to an average rate of 0.03 mT/s. While the difference for SkX(1) and SkX(2), in figures 1(g) and (h), is more obvious than for the chosen magnetic field rates in figure 2, the intensity difference of SkX(1) comparing the rate 3.4 mT/s to the others is of the same magnitude. This means that if even slower rates were used, the difference might

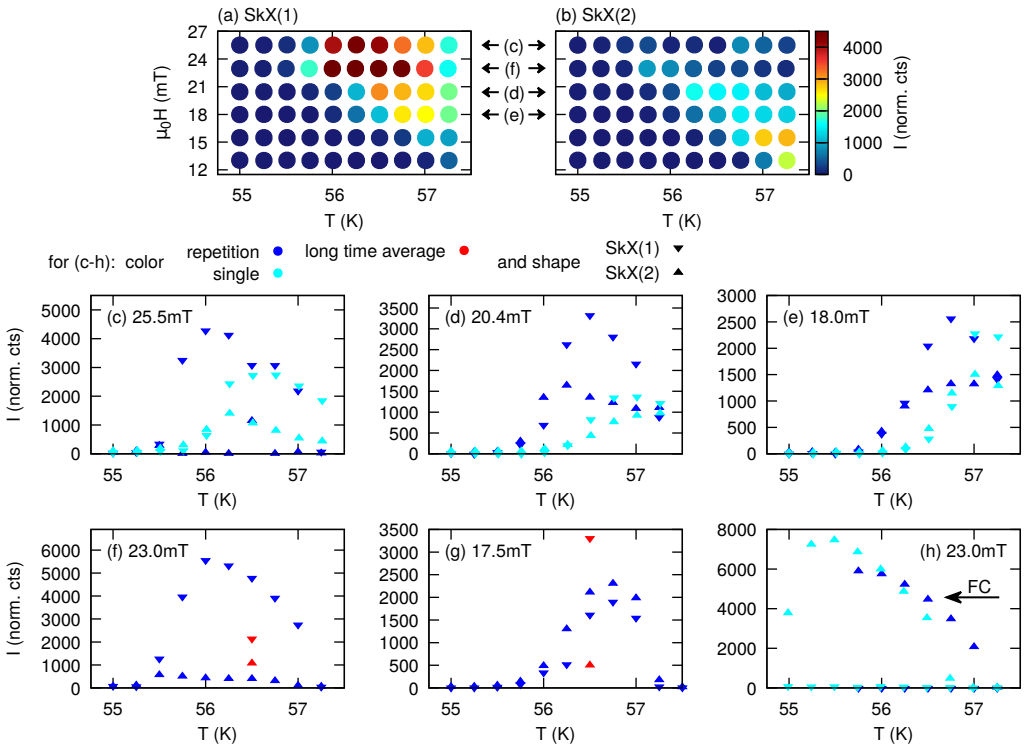

Figure 3. Two-dimensional intensity maps for the SkX(1) (a) and SkX(2) (b) components, obtained by fitting the model function to the azimuthal scattering pattern. Both panels represent results using FW protocols, however, at each configuration three (at $\mu_0 H = 23\,\mathrm{mT}$ five) consecutive measurements were performed, of which the first one is shown. (c-g) The integrated intensities of various constant field scans using the FW protocol. The results from single measurement scans (cyan) and the last measurement of the repetition scans (blue) are displayed for comparison. Furthermore, in (f) and (g) data points were added representing the long time average calculated (red) from time relaxation measurements. (h) For further comparison equivalent graphs obtained using the FC protocol with and without repetitions.

be enhanced further. There is a recent report on the temporal change of the skyrmion-lattice subsequent to a change of the applied magnetic field in thin-film samples of FeGe on the order of 5 s [17]. Due to the measurement time of 60 s employed here, this is not expected to play a major role.

3.2. Impact of temperature sweep rate: Equilibration versus intrinsic stabilization

Ideally a similar experiment on the application of the magnetic field would have been performed for the FC and FW protocol and the influence of the temperature, too. However, our current experimental setup requires at least 600 s for the temperature equilibration for a temperature change of $\Delta T = 3\,\mathrm{K}$ [12], as the temperature sensor is mounted on the same sapphire plate at a finite distance from the sample. In order to minimize the influence from the temperature equilibration the temperature is changed in small steps of $\Delta T = 0.25\,\mathrm{K}$, starting at a temperature outside the skyrmion phase. For each set of steps, we performed one of three different repetition measurements at each temperature step: 1. a single measurement of 60 s, 2. repeat the first measurement two additional times to account for the temperature equilibration or 3. repeat the measurement four times (only used at $\mu_0 H = 17.5$ and 23 mT). The intensity maps for

the first measurement are shown in figures 3(a-b). Comparing these maps with those of the third measurement results [12], the intensity appears slightly reduced at lower-T and increased approaching the phase boundary at higher-T. Apart from the map's constant magnetic field scans in figures 3(c-f) an additional data set measured using the FW protocol with four repetitions at $\mu_0 H = 17.5\,\mathrm{mT}$ is shown in figure 3(g). Despite the small steps in temperature there is still a variation in intensity for each repetition measurement present. The relaxation is largest at the lower and higher-T phase boundaries; however, on the basis of the available measurements, a possible intrinsic temperature dependence of the relaxation behavior cannot be distinguished from the extrinsic influence of the temperature equilibration. Comparing the measurement results in figures 3(c-e) and considering the number of repetitions indicates that longer waiting times for fields $\mu_0 H \gtrsim 18\,\mathrm{mT}$ stabilize SkX(1) over SkX(2) for the FW protocol. However, approaching the lower-H phase boundary the ratio between SkX(1) and SkX(2) decreases and for $\mu_0 H = 17.5\,\mathrm{mT}$ the SkX(2) phase exhibits slightly higher intensities at all temperatures [cf. figure 3(g)]. It is important to note that longer waiting times subsequent to the stabilization of the skyrmion phases cannot make up for incomplete relaxation during the stabilization. This can be seen from the results of time relaxation measurements where the target temperature is set directly from 50 K (FW protocol). The long-time average calculated from the measurements after the temperature equilibration shows significantly different intensities for the skyrmion phases from the respective repetition measurements [cf. figures 3(f) and (g)]. Again, energetic barriers appear to prevent a relaxation of the stabilized skyrmion-lattice.
Figure 3(h) shows two data sets measured using the FC protocol, one without and the other one with four repetitions at $\mu_0 H = 23.0\,\mathrm{mT}$. The difference between these data sets is less compared to those where the FW protocol is used. When entering the skyrmion phase, the waiting times of the repetitions assist with the stabilization process of SkX(2). At lower temperatures (below $T = 56\,\mathrm{K}$), the intensity observed without repetitions exceeds the highest intensities of the other set [cf. figure 3(c)], which is peculiar when only the influence from temperature equilibration is assumed. This suggests a possible intrinsic temperature influence for the FC protocol, too.

4. Conclusion

Previously, we have reported on the influence of certain magnetic field and temperature protocols on the stabilization process. Here, the previously used protocols were varied slightly to investigate the influence of intermediate waiting times. The higher intensity of the ring-like component for the fast ZFC protocol indicates an increase in short-range ordered skyrmion-lattice partitions or rather in the proportion of the system in a glassy state. Yet, close to the phase boundary at $T = 57.25\,\mathrm{K}$ where the SkX(2) phase is dominant, the fast protocol strengthens the stabilization of the SkX(1) phase. The extent to which the increase in SkX(1) may be related to the freezing of the glassy state has to be studied in a future experiment. It becomes, nevertheless, clear in this work that the slow kinetics on the time-scale of a few minutes exists for the ZFC protocol. For the FC and FW protocols, the observation of the temperature equilibration complicates the study of the intrinsic temperature dependence. Based on the repetition measurements, the FC protocol appears to generally require less time for the relaxation; however, the intermediate waiting times still influence the stabilization. Using the FW protocol the system seems to require longer relaxation time. Thus, if the temperature is increased too quickly, the stabilized skyrmion phases will be different. This is even more evident in the comparison of the long-time average from the time relaxation (single step of $\Delta T = 6.5\,\mathrm{K}$) with the repetition measurements providing waiting times at each intermediate temperature step, where the influence of temperature equilibration is negligible. Here, clear differences in the stabilized skyrmion-lattice phases [cf. figures 3(f) and (g)] indicate a glass formation even more prominent compared to the fast ZFC protocol. Minute-time-scale kinetics are therefore expected to exist for the temperature sweep, too. Further studies on the influence of temperature with

specifically designed experiments and optimized sample environments is highly desired. Such an approach is likely to reveal even further insight on the difference between the SkX(1) and SkX(2) phases and enable enhanced control over their respective stabilization.

Acknowledgments
The authors thank Y. Tokura for providing his outstanding insight into the matter at hand and N. Nagaosa for stimulating discussions. This work was partly supported by Grants-In-Aid for Scientific Research (24224009, 15H05458, 15H05883, 16H04007, and 16K13842) from MEXT of Japan. Travel expense for the experiment at QUOKKA at ANSTO was partly sponsored by the General User Program of ISSP-NSL, University of Tokyo.

Appendix A. Details of the slow ZFC phase diagram

(i) The sample is heated up to the paramagnetic temperature ($T = 60\,\mathrm{K}$); (ii) The sample is cooled down to the target measurement temperature, the first one being $T = 57.25\,\mathrm{K}$, with the rate of $2\,\mathrm{K/min}$ under zero magnetic field; (iii) Wait for relatively short time (60 s) for ZFC due to beamtime restriction; (It is expected that this shorter period does not significantly change the obtained phase diagram since, while measuring the lower-field part, $0 \leq \mu_0 H \leq 12.5\,\mathrm{mT}$, the sample reaches its equilibrium temperature target value.) (iv) Magnetic field is set to the target magnetic field, and the SANS pattern is recorded for 1 min. The magnetic field is then set to the next target field increased with the increment of $\mu_0 \Delta H = 2.5\,\mathrm{mT}$. This step is repeated until the maximum field is reached; (v) The magnetic field is turned off ($\mu_0 H = 0$); (vi) The above steps [from (i)] are repeated with the target temperature decreased by a decrement of 0.25 K, until the lowest measurement temperature is reached.

References

[1] Bogdanov A N and Yablonskii D A 1989 *Sov. Phys. JETP* 101
[2] Nagaosa N and Tokura Y 2013 *Nat. Nanotechnol.* **8** 899–911
[3] Mühlbauer S, Binz B, Jonietz F, Pfleiderer C, Rosch A, Neubauer A, Georgii R and Böni P 2009 *Science* **323** 915–919
[4] Yu X, Kanazawa N, Onose Y, Kimoto K, Zhang W, Ishiwata S, Matsui Y and Tokura Y 2011 *Nat. Mater.* **10** 106–109
[5] Münzer W, Neubauer A, Adams T, Mühlbauer S, Franz C, Jonietz F, Georgii R, Böni P, Pedersen B, Schmidt M, Rosch A and Pfleiderer C 2010 *Phys. Rev. B* **81**(4) 041203
[6] Seki S, Kim J H, Inosov D S, Georgii R, Keimer B, Ishiwata S and Tokura Y 2012 *Phys. Rev. B* **85** 220406
[7] Adams T, Chacon A, Wagner M, Bauer A, Brandl G, Pedersen B, Berger H, Lemmens P and Pfleiderer C 2012 *Phys. Rev. Lett.* **108** 237204
[8] Tokunaga Y, Yu X Z, White J S, Rønnow H M, Morikawa D, Taguchi Y and Tokura Y 2015 *Nat. Commun.* **6** 7638–7644
[9] Kezsmarki I, Bordacs S, Milde P, Neuber E, Eng L M, White J S, Rønnow H M, Dewhurst C D, Mochizuki M, Yanai K, Nakamura H, Ehlers D, Tsurkan V and Loidl A 2015 *Nat. Mater.* **14** 1116–1122
[10] Seki S, Yu X Z, Ishiwata S and Tokura Y 2012 *Science* **336** 198–201
[11] Seki S, Ishiwata S and Tokura Y 2012 *Phys. Rev. B* **86** 060403
[12] Makino K, Reim J D, Higashi D, Okuyama D, Sato T J, Nambu Y, Gilbert E P, Booth N, Seki S and Tokura Y 2016 *Preprint 1608.06359*
[13] Miller K H, Xu X S, Berger H, Knowles E S, Arenas D J, Meisel M W and Tanner D B 2010 *Phys. Rev. B* **82** 144107
[14] Gilbert E P, Schulz J C and Noakes T J 2006 *Physica B* **385-86** 1180–1182
[15] Rajeswari J, Huang P, Mancini G F, Murooka Y, Latychevskaia T, McGrouther D, Cantoni M, Baldini E, White J S, Magrez A, Giamarchi T, Rønnow H M and Carbone F 2015 *Proc. Nat. Acad. Sci.* **112** 14212–14217
[16] Qian F, Wilhelm H, Aqeel A, Palstra T T M, Lefering A J E, Brück E H and Pappas C 2016 *Preprint 1607.08177*
[17] Yamasaki Y, Morikawa D, Honda T, Nakao H, Murakami Y, Kanazawa N, Kawasaki M, Arima T and Tokura Y 2015 *Phys. Rev. B* **92** 220421